

SAFETY ANALYSIS REPORT
FOR THE MIT RESEARCH REACTOR (MITR-III)

(Rev. 1)

Nuclear Reactor Laboratory
Massachusetts Institute of Technology
Cambridge, Massachusetts

13.2.1 Maximum Hypothetical Accident

The maximum hypothetical accident (MHA) for the MITR is postulated to be a coolant flow blockage in the fuel element that contains the hottest fuel plate. This could occur as the result of some foreign material falling into the core tank during a refueling. After the primary pumps are started, the object would be swept from the bottom of the tank up to the fuel element nozzle so that flow to the fuel plates was obstructed. In order for this to happen, the foreign material would have to fall through the lower grid plate. This could only occur during a refueling, when a fuel element was removed so that the corresponding position was open. The size of the openings in the lower grid plate would restrict the dimensions of the foreign object to those of a fuel element nozzle. Coolant can pass through either a nozzle's end or side openings. Hence, the foreign object could not block all coolant flow through the nozzle. However, if the material were small enough to enter the triangular entrance in the nozzle, it might possibly block the flow to a maximum of five coolant channels (six plates). Because the two fuel plates on the outer regions of the blocked area will be cooled from one side, the only melting that might occur would involve the inner four fuel plates. It is conservatively assumed that all five coolant channels are blocked and that the entire active portion of the four associated plates melts completely. This is a very conservative assumption because the coolant channels can only be partially blocked because of the geometry of the nozzle. Experience with fuel plate melting both at the Materials Testing Reactor (MTR) and at the Oak Ridge Research Reactor has shown that fuel plate melting because of flow blockage does not propagate beyond the affected flow channels. Although nearby plates were discolored, cooling by the unaffected channels was sufficient to prevent propagation of the melting [13-1, 13-2].

An analysis of fission product release and radiation dose to the off-site population was previously performed by Mull for the MITR-II [13-3]. That analysis was

recently redone by Li both for higher reactor powers and with an updated source term [13-4]. In both analyses, the fission products in the fuel at the time of the accident were assumed to be in equilibrium for the steady-state reactor power. This assumption is conservative for the MITR because the reactor is shut down periodically for maintenance and refueling. Table 13-1 lists the equilibrium fission product activity inventories for reactor powers up to 10 MW. The fission product inventory for 6 MW is used for the current analysis.

13.2.1.1 Containment Source Term

Table 13-2 lists the fission product release fraction from the melted fuel (F_f), the fraction released from the primary coolant system (F_p), and the fraction remaining airborne in the containment atmosphere (F_c). These values, which are used in the current analysis, were taken from Li [13-4] except that the primary coolant system release fraction (F_p) was obtained from a coolant evaporation calculation. Mull [13-3] and Li [13-4] assumed primary coolant release fractions of 0.1 and 0.3 respectively. These values were chosen based on power reactor accident scenarios that involved severe accidents initiated from coolant system failure that eventually lead to core melt [13-5]. The MITR's MHA, which is initiated by coolant channel blockage, does not involve a primary coolant system failure. However, the primary coolant system is not leak tight. Hence volatiles, such as noble gases, may be released to the containment. Also, non-volatile fission product transport from the core tank to the containment is possible through coolant evaporation from the reactor core tank. (Note: Both the loss of volatiles and the evaporative release mechanism for non-volatiles ignore the presence of the reactor top shield lid which is required to be in place if reactor power exceeds 100 kW. The presence of this lid makes the primary system a barrier to fission product release.) A calculation was made to estimate the amount of fission product release to the containment through evaporation during a two hour period [13-6]. Assumptions for this calculation are that the coolant temperature is 60° C, the relative humidity in the upper core tank air space is 10%, the temperature in the air space is 20° C, and the fission products mix uniformly with the primary coolant in the core tank (about 700 gallons). The first assumption specifies the highest possible coolant temperature (LSSS), the second and third assumptions establish the lower bound of air conditions which would result in a higher evaporation rate, and the last assumption conservatively uses only the coolant volume in the core tank instead of the total coolant volume in the primary coolant system. This calculation shows that about 1.6 gallons of

Table 13-1

MITR Core Fission Product Inventory [13-4]

Isotope		Half-life	$\lambda_i(\text{sec}^{-1})$	$Y_i(\%)$	$Q_s^i (\times 10^5 \text{ Ci})$					
					5MW	6MW	7MW	8MW	9MW	10MW
Kr	85m	4.36h	4.41E-5	1.5	0.6490	0.7788	0.9086	1.0384	1.1682	1.3000
	87	78m	1.48E-4	2.7	1.1700	1.4040	1.6380	1.8720	2.1060	2.3400
	88	2.77h	6.95E-5	3.7	1.6000	1.9200	2.2400	2.5600	2.8800	3.2000
Xe	131m	12.0d	6.68E-7	0.03	0.0130	0.0156	0.0182	0.0208	0.0234	0.0260
	133m	2.3d	3.49E-6	0.16	0.0692	0.0830	0.0969	0.1107	0.1246	0.1380
	133	5.27d	1.52E-6	6.5	2.8100	3.3720	3.9340	4.4960	5.0580	5.6200
	135m	15.6m	7.40E-4	1.8	0.7780	0.9336	1.0892	1.2448	1.4004	1.5600
	135	9.13h	2.11E-5	6.2	0.4130	0.4956	0.5782	0.6608	0.7434	0.8260
	138	17m	6.79E-4	5.5	2.3800	2.8560	3.3320	3.8080	4.2840	4.7600
I	131	8.05d	9.96E-7	2.9	1.2500	1.5000	1.7500	2.000	2.2500	2.5100
	132	2.4h	8.02E-5	4.4	1.9000	2.2800	2.6600	3.0400	3.4200	3.8100
	133	20.8h	9.25E-6	6.5	2.8100	3.3720	3.9340	4.4960	5.0580	5.6200
	134	52.5m	2.20E-5	7.6	3.2900	3.9480	4.6060	5.2640	5.9220	6.5700
	135	6.68h	2.89E-5	5.9	2.5500	3.0600	3.5700	4.0800	4.5900	5.1000
Br	83	2.4h	8.02E-5	0.48	0.2080	0.2496	0.2912	0.3328	0.3744	0.4150
	84	30m	3.85E-5	1.1	0.4760	0.5712	0.6664	0.7616	0.8568	0.9510
Cs	134	2.0y	1.10E-8	0.0*	2.8600	3.4320	4.0040	4.5760	5.1480	5.7200
	136	13d	6.17E-7	0.006*	0.4140	0.4968	0.5796	0.6624	0.7452	0.8280
	137	26.6y	8.27E-10	5.9	2.3100	2.7720	3.2340	3.6960	4.1580	4.6200
Rb	86	19.5d	4.11E-7	2.8E-5*	0.6120	0.7344	0.8568	0.9792	1.1016	1.2200
Te	127m	90d	8.82E-8	0.056	0.0242	0.0290	0.0339	0.0387	0.0436	0.0484
	127	9.3h	2.07E-5	0.25	0.1080	0.1296	0.1512	0.1728	0.1944	0.2160
	129m	33d	2.43E-7	0.34	0.1470	0.1764	0.2058	0.2352	0.2646	0.2940
	129	72m	1.60E-4	1.0	0.4320	0.5184	0.6048	0.6912	0.7776	0.8650
	131m	30h	6.42E-5	0.44	0.1900	0.2280	0.2660	0.3040	0.3420	0.3810
	131	24.8m	4.66E-4	2.9	1.2500	1.500	1.7500	2.000	2.2500	2.5100
	132	77h	2.50E-6	4.4	1.9000	2.2800	2.6600	3.0400	3.4200	3.8100
	133m	63m	1.83E-4	4.6	1.9900	2.3880	2.7860	3.1840	3.5820	3.9800
	134	44m	2.63E-4	6.7	2.9000	3.4800	4.0600	4.6400	5.2200	5.8000
Sr	91	97h	2.99e-5	5.9	2.5500	3.0600	3.5700	4.0800	4.5900	5.1000
Ba	140	12.8d	6.27E-7	6.3	2.7200	3.2640	3.8080	4.3520	4.8960	5.4500

Table 13-1 (cont'd)

MITR Core Fission Product Inventory [13-4]

Isotope		Half-life	$\lambda_i(\text{sec}^{-1})$	$Y_i(\%)$	$Q_s^i (\times 10^5 \text{ Ci})$					
					5MW	6MW	7MW	8MW	9MW	10MW
Ru	103	41d	1.96E-7	2.9	1.2500	1.5000	1.7500	2.0000	2.2500	2.5100
	105	4.5h	4.28E-5	0.9	0.3890	0.4668	0.5446	0.6224	0.7002	0.7790
	106	1.0y	2.20E-8	0.38	0.1640	0.1968	0.2296	0.2624	0.2952	0.3290
Rh	103	36.5h	5.27E-6	0.9	0.3890	0.4668	0.5446	0.6224	0.7002	0.7790
Tc	99m	6.04h	3.19E-5	0.6	0.2590	0.3108	0.3626	0.4144	0.4662	0.5190
Mo	99	67h	2.88E-6	6.1	2.6400	3.1680	3.6960	4.2240	4.7520	5.2800
Sb	127	93h	2.07E-6	0.25	0.1080	0.1296	0.1512	0.1728	0.1944	0.2160
	129	4.6h	4.32E-5	1.0	4.3200	5.1840	6.0480	6.9120	7.7760	8.6500
Nd	147	11.3d	7.10E-7	2.6	1.1200	1.3440	1.5680	1.7920	2.0160	2.2500
La	140	40.2h	4.79E-6	6.3	2.7200	3.2640	3.8080	4.3520	4.8960	5.4500
Ce	141	32d	2.51E-7	6.0	2.5900	3.1080	3.6260	4.1440	4.6620	5.1900
	143	32h	6.01E-6	6.2	2.6800	3.2160	3.7520	4.2880	4.8240	5.3600
	144	290d	2.76E-8	6.1	2.6400	3.1680	3.6960	4.2240	4.7520	5.2800
Zr	95	63d	1.27E-7	6.4	2.7700	3.3240	3.8780	4.4320	4.9860	5.5400
	97	17h	1.13E-5	6.2	2.6800	3.2160	3.7520	4.2880	4.8240	5.3600
Nb	95	35d	2.29E-7	6.4	2.7700	3.3240	3.8780	4.4320	4.9860	5.5400

Table 13-2Fission Product Release Fractions

Fission Product	Fraction Released from the Melted Fuel F_f	Fraction Released from the Primary Coolant System F_p^*	Fraction Remaining Airborne in the Containment Atmosphere F_c
Noble Gases	1.0	1.0	1.0
I	0.9	0.03	0.3
Cs	0.9	0.03	0.3
Te	0.23	0.03	0.9
Sr	0.01	0.03	0.9
Ba	0.01	0.03	0.9
Ru	0.01	0.03	0.9
La	0.0001	0.03	0.9
Ce	0.0001	0.03	0.9
Others	0.0001	0.03	0.9

* Based on coolant evaporation calculation.

primary coolant would be lost through evaporation during a two-hour period. This is equivalent to about 0.3% of the primary coolant in the core tank. The actual fraction would

be lower because both the pool of water above the core and the presence of the reactor top shield lid would limit the release rate. A coolant system release fraction of 3% is adopted to conservatively bound the non-volatile fission product release. In addition, it is assumed that 100% of the noble gases are released to the containment.

Because the MITR has no containment spray or other engineered safeguards features to reduce the quantity of fission products in the containment atmosphere, depletion of the radioactive isotopes released to the containment occurs through natural processes. These include agglomeration and sedimentation. Agglomeration is the process by which the size distribution of airborne particulate tends to shift with time to larger sizes until an equilibrium condition is reached. This process affects sedimentation which is deposition because of gravitation. The noble gases are not expected to undergo either of these depletion process and thus they remain in the containment atmosphere.

The fission product activities in the containment atmosphere will vary with time. Activity initially increases as more fission products are released from the melted plates. A maximum occurs when a balance is reached with the depletion processes described above. The activity then starts to decrease because the natural depletion processes and leakage continue while the source is finite. It was assumed for the analysis that the containment activity was at its maximum (instantaneous release) from the beginning of the accident and the natural depletion processes started to take place simultaneously. In this analysis, fission product leakage from the containment was neglected as a removal mechanism. During the two hour period, it was assumed that the depletion for iodine and cesium was 70%, and that depletion for the other non-volatile elements was 10% [13-4].

13.2.1.2 Off-Site Radiation Dose Calculations

The following approaches were used to evaluate effects of the major release paths to the exclusion area during the maximum hypothetical accident:

- a) An analysis was made to determine the atmospheric release from the containment building. The radiation doses that resulted from leakage (including external gamma dose from plume, beta dose, and thyroid dose) were calculated using a standard Gaussian diffusion model and local meteorological data.
- b) Gamma radiation reaching the boundary area by direct penetration of the containment shell was calculated using standard shielding calculations. A Compton scattering model was developed and applied to photon scattering from the steel containment roof.
- c) An analysis for radiation streaming was performed for the truck airlock which is the largest containment penetration.

13.2.1.3 Atmospheric Release

There are two paths for the fission products in the containment building to be released to the outside. One is a controlled release through the stack via the containment's pressure relief system. The other is containment leakage which is not controllable.

The containment building was designed to withstand internal pressures up to 2.0 psi above atmospheric and 0.1 psi lower than atmospheric. The building is normally maintained at a pressure slightly less than atmospheric in order to prevent out-leakage. If high radiation levels were detected by the plenum gas or particulate monitors, the building ventilation system's intake and exhaust fans would stop and both isolation dampers would close automatically. The maximum permissible leakage rate is 1% of the building volume per day per psi of overpressure. An integral air leakage test of the containment building is performed periodically to ensure that this criterion is satisfied. It is assumed conservatively in the containment leakage calculation that the containment

pressure remains constant at 2.0 psig during the accident and that this results in a continuous release of the fission products to the environment at the maximum permissible leakage rate.

The containment building is equipped with a pressure relief system which consists of a blower, roughing filters, two high-efficiency absolute particulate air filters, and an activated charcoal filter for removal of elemental iodine (See Section 6.5.4.2 of this report.). The volumetric flow rate through this system was obtained from experimental data [13-7]. The fractions of radionuclides penetrating through the filters of the pressure relief system are: 100% of noble gases and bromine, 5% of iodine, 50% of all the others [13-4].

Atmospheric dispersion of a pollutant is primarily dependent on (1) meteorological conditions such as ambient temperature, wind speed, time of day, insolation, and cloud cover (atmospheric stability), and (2) pollutant stack emission parameters such as effluent velocity and temperature. The stability of the atmosphere is determined by the atmospheric thermal gradient, which is called the lapse rate. Neutral stability exists for a vertical temperature gradient of $-1\text{ }^{\circ}\text{C}/100\text{ meters}$. Unstable conditions with lapse rates greater than $-1\text{ }^{\circ}\text{C}/100\text{ m}$ add to the buoyancy of an emission, and stable conditions (lapse rates less than $-1\text{ }^{\circ}\text{C}/100\text{ m}$) tend to inhibit downward vertical motion of the pollutant gases (plume). Dispersion from an elevated source (stack) is affected by the mixing and dilution of polluted gases with the atmosphere.

For a stack release, the maximum ground-level concentration in a sector may occur beyond the exclusion area boundary distance. Therefore, for stack releases, the atmospheric relative concentration values are calculated at various distances. Values of dispersion coefficients, which depend on the downwind distance and the atmospheric stability category, can be determined from the Pasquill curves [13-8] (a set of diffusion coefficient curves versus plume travel distance). In most references, the dispersion coefficients are given as a set of curves over the range of 10^2 to 10^5 meters. It is

impossible to extrapolate these curves accurately to the range of the MITR's exclusion area distance, 8 to 21 meters. One alternative is to use the interpolation formulas for σ_y and σ_z developed by Briggs which fit the Pasquill curves [13-9].

The meteorological data needed for the atmospheric relative concentration calculation include wind speed, wind direction, and a measure of atmospheric stability. The meteorological data used in this report were recorded at the Boston Station, MA 240BS 93-95. The wind speed data are expressed in the units of knots, where one knot equals 1853 meters/hour. The annual average wind speed for each stability category in the Boston area is listed in Table 13-3. It is shown that class D (neutral stability) is the most frequent stability condition, accounting for about 74% of the total events.

For release from the stack, the more unstable an atmospheric condition, the more a pollutant will be deposited in a shorter range with a higher concentration. In contrast, a more stable atmosphere would disperse the pollutant over a wider range and thus result in a lower concentration. From the meteorological data for the Boston area, it was found that the dose rates at 8 and 21 m are negligible based on class C, D, and E which account for most of the atmospheric conditions (frequency of 94%).

For containment release, the model ("exact" model) proposed in the U.S. NRC Regulatory Guide 1.145 is adopted [13-10]. Figure 13.1 shows the comparison of atmospheric relative concentrations for class A, B, C, D, E, and F versus distance. Class F represents a conservative estimate for both the site boundary and the restricted area and is therefore adopted as the limiting case of the ground release. It is noted that the calculated doses for class F stability would give a conservative estimate of the release with frequency greater than 99%. [13-4]

Table 13-3Wind Speed for Each Stability Category (knots) Averaged Over All Directions

	A	B	C	D	E	F
N	0.0	5.4	7.7	10.3	7.2	4.8
NNE	0.0	6.1	8.2	11.0	6.3	4.5
NE	0.0	5.0	8.4	12.4	6.0	3.8
ENE	5.0	6.3	9.6	11.8	6.5	3.8
E	5.0	6.6	9.8	10.4	6.8	3.8
ESE	5.0	6.2	9.6	10.8	6.9	3.8
SE	4.5	7.1	8.4	9.4	6.3	4.1
SSE	5.0	5.8	7.3	9.0	6.3	4.4
S	1.0	5.0	8.5	10.6	6.6	4.8
SSW	4.5	5.6	9.1	12.1	7.4	5.1
SW	5.0	6.6	9.9	12.0	7.9	5.1
WSW	0.0	6.5	9.7	12.0	8.1	5.3
W	5.0	6.7	9.7	13.2	8.4	5.0
WNW	3.0	6.7	9.0	13.4	8.4	5.0
NW	5.0	6.1	10.0	13.2	8.3	5.0
NNW	4.0	6.5	9.0	12.5	8.2	4.6
Average	3.8	6.4	9.2	11.9	7.7	4.6
relative freq. (%)	0.00823	1.8254	8.3007	73.9423	12.0338	3.8154

* A-Extremely unstable, B-Moderately unstable, C-Slightly unstable, D-Neutral
E-Slightly stable, F-Moderately stable.

13.2.1.4 Direct and Scattered Gamma Dose from Contained Source

Those radionuclides that are retained in the containment building constitute a source of gamma radiation. The gamma dose at the exclusion boundary consists of direct gamma dose, scattered gamma dose, and the gamma dose through the truck lock. Separate calculations were performed and the results summed for the two parts of the containment building (the sides which are shielded by both concrete and steel and the dome which is shielded only by steel as described in Section 6.5.1 of this report) and the truck lock. The truck lock is an eight-meter long rectangular steel passage closed at both ends by pneumatically sealed doors. Each door consists of a steel framework that is covered by steel plates on both sides. The two sides of the truck lock are shielded by concrete walls 0.5 meters thick while the front and top are not shielded. The radiation reaching the truck lock was treated as a point source located at the center of the inner surface of the inner door.

13.2.1.5 Conclusion for the Maximum Hypothetical Accident

A summary of the calculated results for the MITR MHA is given in Table 13-4. Even with the conservative assumptions of the release fractions and fission product equilibrium, the estimated external doses to an individual located at the nearest point of public occupancy during the first two hours of the MITR MHA are 197 mrem at 8 m (back fence) and 247 mrem at 21 m (front fence) to the whole body. The maximum whole body dose is 300 mrem at 16 m. The internal doses are 135 mrem and 134 mrem to the thyroid for 8 m and 21 m, respectively.

Concentration of Ar-41 is predicted to be 1.79×10^{-3} $\mu\text{Ci/ml}$ for 6 MW. This estimate is extrapolated from measurements performed for the MITR at 5 MW. Compared to fission products released from the fuel, this concentration is lower by a factor of 5 to 7. Therefore, the contribution of Ar-41 to the off-site dose is negligible [13-4].

Table 13-4

Estimated Doses from all Modes of Radiation Release During a MITR
Maximum Hypothetical Accident [13-4]

Component of the Dose	Dose (mrem) (c)	
	8 m (a)	21 m (b)
Whole body:		
Containment Leakage	12	12
Steel Dome Penetration	3	25
Shadow Shield Penetration	44	21
Air Scattering	57	75
Steel Scattering	87	114
Total (d)	197	247
Thyroid:		
Containment Leakage	135	134

(a) Boundary of restricted area

(b) Nearest point of public occupancy

(c) Calculation assumes that radiation emergency plan for protection of the public will be implemented in less than two hours.

(d) The maximum whole body dose is 300 mrem at 16 m.

References

- 13-1 J.W. Dykes et al., A Summary of the 1962 Fuel Element Fission Break in the MTR, IDO-17064, February 1965.
- 13-2 W.H. Tabor, Fuel Plate Melting at the Oak Ridge Research Reactor, ANS Transactions 8 Suppl., 36, July 1965.
- 13-3 R.F. Mull, Exclusion Area Radiation Release During the MIT Reactor Design Basis Accident, S.M. Thesis, Nuclear Engineering Department, MIT, May 1983.
- 13-4 Q. Li, Estimate of Radiation Release for MIT Research Reactor During Design Basis Accident, S.M. Thesis, Nuclear Engineering Department, MIT, May 1998.
- 13-5 U.S. Nuclear Regulatory Commission, Severe Accident Risks: An Assessment for Five U.S. Nuclear Power Plants, NUREG-1150, June 1989.
- 13-6 File Memo (MITR Coolant System Release Fraction during the MHA, March 1999).
- 13-7 J. Gosnell, Modification of Pressure Relief System, Technical Report.
- 13-8 F.A. Gifford, An Outline of Theories of Diffusion in the Lower Layers of the Atmosphere, Meteorology and Atomic Energy, July 1968.
- 13-9 Reactor Safety Study, Calculations of Reactor Accident Consequences, WASH-1400, October 1975.
- 13-10 Atmospheric Dispersion Models for Potential Accident Consequence Assessments at Nuclear Power Plants, U.S. NRC Regulatory Guide 1.145, November 1982.
- 13-11 Safety Analysis Report for the MIT Research Reactor (MITR-II), MITNE-115, October 1970.
- 13-12 W. Woodruff, A Kinetics and Thermal-Hydraulics Capability for the Analysis of Research Reactors, Nuclear Technology, pp. 196-206, Vol. 64, Feb. 1984.
- 13-13 T.J. Thompson and J.G. Beckerley, The Technology of Nuclear Reactor Safety, Vol. 1, MIT Press, 1964.
- 13-14 File Memo (MITR Step Reactivity Insertion Transient, June 1999).
- 13-15 File Memo (Ramp Reactivity Insertion Calculations for MITR-III, April 1999).

- 13-16 L.-W. Hu and J. A. Bernard, "Development and Benchmarking of a Thermal-Hydraulics Code for the MIT Nuclear Research Reactor," Proceedings of the ANS Joint International Conference on Mathematical Methods and Super-Computing for Nuclear Applications, pp 1117-1127, Saratoga, NY, Oct. 5-7, 1997.
- 13-17 MITR-II Startup Report, MITNE-198, February 1977.
- 13-18 G. Allen, Jr., Aspects of A Seismic Study of the MITR, S.M. Thesis, Department of Nuclear Engineering, MIT, May 1971.
- 13-19 File Memo (Accident Analysis for One Shim Blade Drop, March 1999).
- 13-20 G. Walgenwitz, Response of the MIT Nuclear Reactor Top Lid to a Fuel Transfer Cask Drop Impact, MIT/NRL Special Report, June 1995.
- 13-21 File Memo (Spill of Heavy Water, June 1999).
- 13-22 T.B. Fowler, D.R. Vondy, G.W. Cunningham, "Nuclear Reactor Core Analysis Code: CITATION", ORNL-TM-2496, Rev.2, 1971.

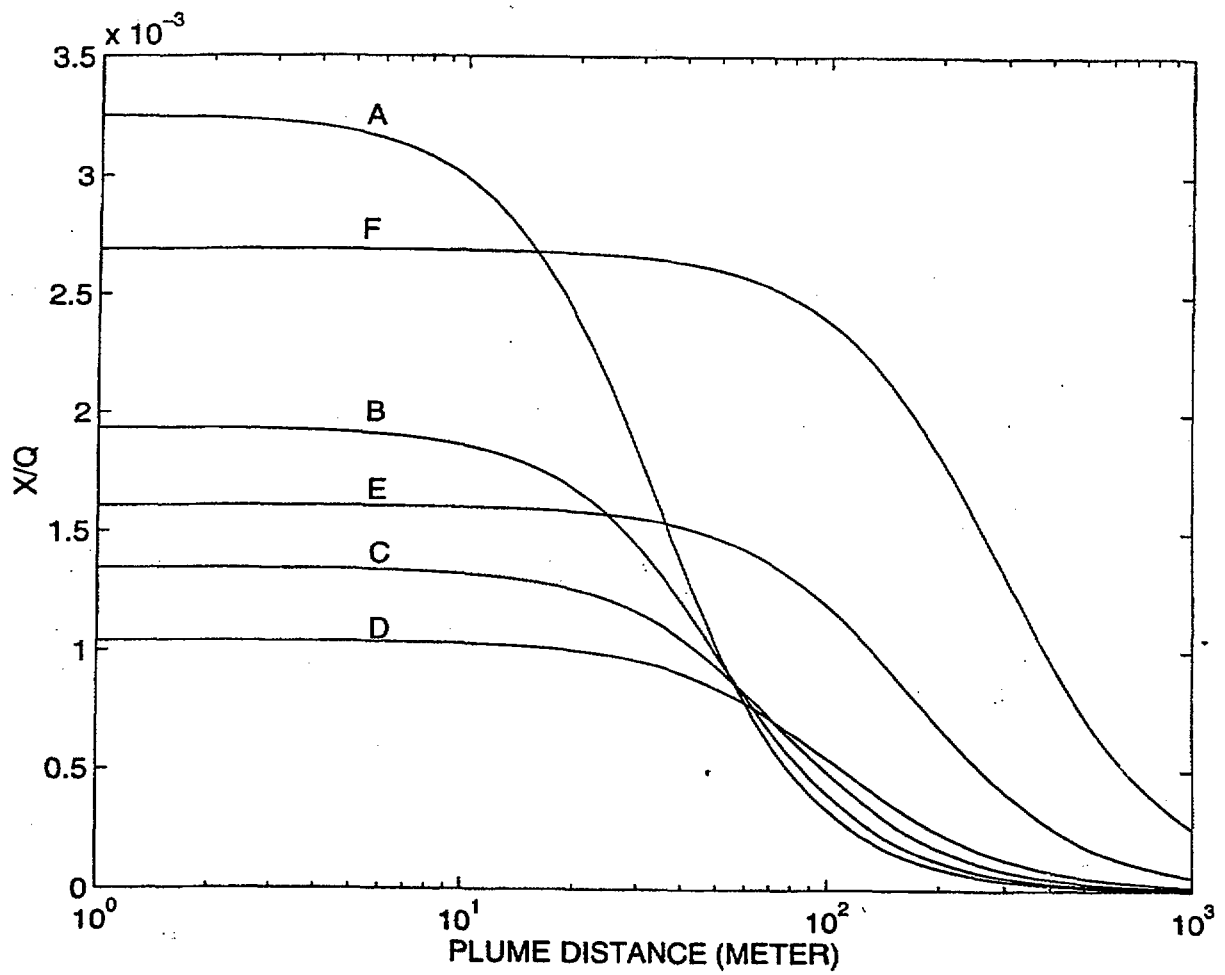


Figure 13-1 Relative Atmospheric Concentrations (X/Q) as a Function of Plume Distance for Each Atmospheric Condition from Containment Leakage using the "Exact" Model. [13-4]